Constraining RS Models by Future Flavor and Collider Measurements: A Snowmass Whitepaper

Kaustubh Agashe,[1] Martin Bauer,[2,3] Florian Goertz,[4] Seung J. Lee,[5,6] Luca Vecchi,[1] Lian-Tao Wang,[3,7] and Felix Yu[2]

[1] *Maryland Center For Fundamental Physics, Department of Physics, University of Maryland, College Park, MD 20742, USA*
[2] *Fermi National Accelerator Laboratory, P.O. Box 500, Batavia, IL 60510, USA*
[3] *Enrico Fermi Institute, University of Chicago, Chicago, IL 60637, USA*
[4] *Institute for Theoretical Physics, ETH Zurich, 8093 Zurich, Switzerland*
[5] *Department of Physics, Korea Advanced Institute of Science and Technology, 335 Gwahak-ro, Yuseong-gu, Daejeon 305-701, Korea*
[6] *School of Physics, Korea Institute for Advanced Study, Seoul 130-722, Korea*
[7] *KICP and Dept. of Physics, University of Chicago, 5640 S. Ellis Ave., Chicago, IL 60637, USA*

(Dated: October 4, 2013)

Randall-Sundrum models are models of quark flavor, because they explain the hierarchies in the quark masses and mixings in terms of $\mathcal{O}(1)$ localization parameters of extra dimensional wavefunctions. The same small numbers which generate the light quark masses suppress contributions to flavor violating tree level amplitudes. In this note we update universal constraints from electroweak precision parameters and demonstrate how future measurements of flavor violation in ultra rare decay channels of Kaons and B mesons will constrain the parameter space of this type of models. We show how collider signatures are correlated with these flavor measurements and compute projected limits for direct searches at the 14 TeV LHC run, a 14 TeV LHC luminosity upgrade, a 33 TeV LHC energy upgrade, and a potential 100 TeV machine. We further discuss the effects of a warped model of leptons in future measurements of lepton flavor violation.

I. INTRODUCTION

While scales of quark flavor violation in generic new physics (NP) models are already constrained to $\Lambda_{\rm NP} > 100-10^4$ TeV [1], flavor violating processes in the bulk Randall-Sundrum (RS) model are screened by the RS-GIM mechanism, resulting in a relatively weak bound on the new physics scale of $\Lambda_{\rm RS} \lesssim 10$ TeV [2–5].

In the minimal realization of these models, all Standard Model (SM) fields propagate in the five dimensional (5D) bulk, while the Higgs is confined on or close to the infrared (IR) brane. In this setup, there arise large contributions to the oblique T parameter, which is sensitive to the mixing of the electroweak gauge bosons and their heavy excitations. Similarly, there are sizable positive corrections to the $Zb_L\bar{b}_L$ coupling due to both mixing of the Z boson with its Kaluza-Klein (KK) excitations as well as non-negligible mixing of the fermion KK modes with the bottom quark zero mode [6].

It is possible to capture the physics of RS models by a dual description, in which the above effects can be understood in terms of the mixing of elementary fields with heavy composite resonances of a new strongly coupled nearly-conformal interaction with a confining phase at $\Lambda_{\rm RS} < 10$ TeV. In this language, the 5D bulk gauge group corresponds to a *global* symmetry of the composite sector and only the residual symmetry group on the UV brane is gauged in the dual theory. This realization allows us to understand how the minimal bulk RS model fails to protect the T parameter from large corrections, because the SM bulk gauge group does not contain an approximate custodial $SU(2)_L \times SU(2)_R$ symmetry. An enlarged bulk gauge group with the appropriate choice of boundary conditions can therefore protect the T parameter. In the KK decomposed theory, this manifests itself through a cancellation between the KK modes of the $SU(2)_L$ gauge bosons and their $SU(2)_R$ equivalents. The tension in the $Zb\bar{b}$ couplings can also be resolved, if the down type quarks are demanded to transform under a suitable $SU(2)_L \times SU(2)_R$ representation in order to suppress both the corrections from gauge bosons, as well as from fermion mixing. Before the discovery of the 126 GeV scalar and in absence of such a symmetry, the large positive contributions to T and $g^Z_{\bar{b}_L b_L}$ in the minimal model could also be interpreted as a sign of a heavy SM-like Higgs boson, but in view of the most recent electroweak parameter fit, the T parameter sets a definitive bound of $\Lambda_{\rm RS} > 5$ TeV. We will therefore consider the minimal model only for very high mass scales $\Lambda_{\rm RS} \in [5, 10]$ TeV, and for contrast, we will also analyze a custodially protected bulk RS model for mass scales of $\Lambda_{\rm RS} \in [2, 10]$ TeV. Strong constraints from CP violation in the $K - \bar{K}$ system push the compositeness scale $\Lambda_{\rm RS} > 8$ TeV independent of the bounds from electroweak precision measurements. We will consider models in which this constraint is accidentally fulfilled by an order 1% fine-tuning, but also discuss models with a UV scale large enough to evade this bound.

Section II will contain a short introduction to the generation of flavor hierarchies in RS models, and introduce the parameter space of the models discussed in this note. In Section III, existing constraints on the parameter space from electroweak precision tests and CP violating observables will be quantified and the role of tree vs. loop mediated flavor violating processes in the RS model will be discussed. The main part of this paper is a compilation of the reach of the next generation flavor experiments in terms of the model parameter space, which will be given in Section IV for quark flavor observables. In Section V we will argue how these experiments provide a unique possibility to constrain or discover an RS type model, because they probe a complementary parameter space to the reach of LHC or future collider searches. Section VI discusses the anarchic model building considerations focusing on the leptons and Section VII discusses future measurements and constraints arising from lepton flavor observables. We conclude in Section VIII.

II. WARPED EXTRA DIMENSIONS

In order to test the RS setup we would like to overconstrain its parameters and search for possible inconsistencies. Here we will only introduce the most important concepts and relations for this purpose and refer to Refs. [4, 5, 7] for a detailed setup of the models under consideration. We will parametrize the extra dimension by the dimensionless variable $t \in [\epsilon, 1]$. The 5D metric reads

$$ds^2 = \frac{\epsilon^2}{t^2}\left(\eta_{\mu\nu}\, dx^\mu dx^\nu - \frac{1}{M_{\rm KK}^2} dt^2\right), \tag{1}$$

leading to a suppression of mass scales at the IR boundary at $t = 1$ by the *warp factor* ϵ. This offers a solution to the hierarchy problem, if the Higgs sector is localized at this brane and if we chose ϵ to be given by the ratio between the Planck and the electroweak scale, $\epsilon = \Lambda_{\rm Weak}/\Lambda_{\rm Pl}$. Above, $M_{\rm KK} = k\epsilon$ is the new physics scale, or *KK scale*, and k is the curvature of the Anti-de Sitter (AdS) space. From here on, we will identify $\Lambda_{\rm RS} \equiv M_{\rm KK}$. If r denotes the radius of the extra dimension, its size can also be described by its dimensionless *volume* $L = kr\,\pi \sim 36$, where $\epsilon = e^{-L}$.

Besides the two new universal parameters, L, which is fixed by the warped geometry to address the hierarchy problem, and $M_{\rm KK}$, the 5D Lagrangian of the minimal RS model features nine quark vector mass parameters, given by the eigenvalues of the hermitian matrices $\boldsymbol{M}_{Q,u,d}$, in which the subscript Q denotes the mass for the $SU(2)_L$ doublet and u, d the masses of the up-type and down-type singlets. After KK decomposition these will determine the localization of the zero modes along the fifth dimension and since they are all of the order of the curvature scale we will refer to the dimensionless ratios $c_{Q_i} = M_{Q_i}/k$, $c_{q_i} = -M_{q_i}/k$ as the *localization parameters*. The custodial extension with an appropriate embedding of the fermion content requires additional matter fields and has in principle 12 quark localization parameters. As was shown in Ref. [7], however, the cancellation of the corrections to the $Zb_L\bar{b}_L$ vertex requires the three additional parameters to be fixed by the SM fields' localization, so we will not treat them as free parameters. In addition, there are Yukawa couplings between the 5D quarks and the Higgs, $\boldsymbol{Y_U}, \boldsymbol{Y_D}$. These cannot be simultaneously diagonalized together with the 5D quark mass matrices and therefore they introduce in principle 36 new free parameters. The physical masses of the quarks as well as the mixing angles of the CKM matrix impose nine constraints in total on this parameter space.

Just like in the SM, hierarchical entries in the Yukawa matrices can generate the observed structure in the physical quark masses and mixings in the CKM matrix. A very appealing feature of the AdS metric is however, that the overlap of the zero modes of the 5D fields with the IR brane and therefore with the Higgs depends exponentially on the localization parameters, and can be expressed by the so-called *profile function*

$$F(c) = \mathrm{sgn}(\cos \pi c) \sqrt{\frac{1+2c}{1-\epsilon^{1+2c}}}\,. \tag{2}$$

As a result, an order one splitting between the localization parameters can explain the hierarchies in quark masses and mixings even for anarchic $\mathcal{O}(1)$ Yukawa couplings. Following this ansatz, the physical quark masses are given by the eigenvalues of the effective 4D Yukawa matrices[1]

$$\boldsymbol{Y}_q^{\rm eff} = \mathrm{diag}\left[F(c_{Q_i})\right] \boldsymbol{Y}_q \mathrm{diag}\left[F(c_{q_i})\right] = \boldsymbol{U}_q\, \boldsymbol{\lambda}_q\, \boldsymbol{W}_q^\dagger\,, \tag{3}$$

in which the unitary matrices

$$(U_q)_{ij} \sim \begin{cases} \dfrac{F(c_{Q_i})}{F(c_{Q_j})}\,; & i \le j\,, \\ \dfrac{F(c_{Q_j})}{F(c_{Q_i})}\,; & i > j\,, \end{cases} \qquad (W_q)_{ij} \sim \begin{cases} \dfrac{F(c_{q_i})}{F(c_{q_j})}\,; & i \le j\,, \\ \dfrac{F(c_{q_j})}{F(c_{q_i})}\,; & i > j\,, \end{cases} \tag{4}$$

rotate from the interaction to the mass eigenbasis, so that $\boldsymbol{\lambda}_q$ is a diagonal matrix with $(\lambda_q)_{ii} = \sqrt{2} m_{q_i}/v$. The masses are then given by

$$m_{u_i} = Y_* \frac{v}{\sqrt{2}} \left|F(c_{Q_i})\right| \left|F(c_{u_i})\right|\,, \qquad m_{d_i} = Y_* \frac{v}{\sqrt{2}} \left|F(c_{Q_i})\right| \left|F(c_{d_i})\right|\,, \tag{5}$$

where $Y_* = f_i(\,(Y_q)_{kl})$ is a flavor dependent function of $\mathcal{O}(1)$ matrix elements [4]. Following the philosophy that the Yukawa couplings add no flavor structure, Y_* should only be sensitive to the average absolute value of $|(Y_q)_{kl}|$, decreasing the 36 new Yukawa parameters effectively to 2. In the following we will moreover assume this average in the down sector to be equal to that in the up sector, leaving us with only one effective parameter from the Yukawa couplings. The expressions (4) and (5) follow from a Froggatt-Nielsen analysis [8] and are, to leading order, independent of the KK scale $M_{\rm KK}$. Equation (5) provides six constraints on the parameter space of the RS model and two further constraints can be derived from two of the Wolfenstein parameters,

$$A \sim \frac{|F(c_{Q_2})|^3}{|F(c_{Q_1})|^2 |F(c_{Q_3})|}\,, \qquad \lambda \sim \frac{|F(c_{Q_1})|}{|F(c_{Q_2})|}\,, \tag{6}$$

while ρ and η only depend on the Yukawa matrices. As indicated above, in the anarchic RS model, we will only treat the average absolute value of the Yukawa-matrix entries as a free model parameter. Therefore, six physical masses and two Wolfenstein parameters constrain the average size of the Yukawa couplings and the nine quark localizations. This leaves only one free localization parameter, which will determine the relative global localization of the right handed

[1] Even though the plots in this work show the result of exact calculations, we will refer to the relevant studies [4, 5, 7] for the exact formulas and restrict the discussion here to approximations to leading order in $v/M_{\rm KK}$ and quark mass hierarchies.

to the left handed zero modes and we can therefore describe the anarchic (both the minimal and the custodially protected) RS model by

$$M_{\rm KK}, \qquad F(c_{u_3}) \qquad \text{and} \qquad Y_*. \tag{7}$$

The other parameters are then fixed to *leading order* in $v/M_{\rm KK}$ and the quark mass hierarchies, and we are left with only 3 additional inputs, increasing the predictivity with respect to many other (non-anarchic) models beyond the SM. It is remarkable that the light quark profiles, which are fixed by their masses, also determine the size of the couplings to KK gauge boson excitations as well as non-SM couplings to the Z and the $W^\pm$. Therefore, flavor-changing neutral currents (FCNCs) are not only suppressed by powers of the new physics scale $M_{\rm KK}$, but also by the masses of the involved quarks. This is the so-called RS-GIM mechanism and a particularly attractive feature of RS models. Integrating out the contributions from the exchange of all KK excitations of the photon leads for example to the Hamiltonian

$$\begin{aligned}\mathcal{H}_{\rm eff}^{(\gamma)} = \frac{2\pi\alpha}{M_{\rm KK}^2} \sum_{q,q'=u,d} S(\bar{q}_i, q_j; \bar{q}'_k, q'_l)\, Q_q Q_{q'} \Big\{ & \frac{1}{2L}\,(\bar{q}\gamma^\mu q)\,(\bar{q}'\gamma_\mu q') \\ & - 2\left(\bar{q}_L\gamma^\mu \mathbf{\Delta}'_Q q_L + \bar{q}_R\gamma^\mu \mathbf{\Delta}'_q q_R\right)(\bar{q}'\gamma_\mu q') \\ & + 2L\big(\bar{q}_L\gamma^\mu \widetilde{\mathbf{\Delta}}_Q q_L + \bar{q}_R\gamma^\mu \widetilde{\mathbf{\Delta}}_q q_R\big) \otimes \big(\bar{q}'_L\gamma_\mu \widetilde{\mathbf{\Delta}}_{Q'} q'_L + \bar{q}'_R\gamma_\mu \widetilde{\mathbf{\Delta}}_{q'} q'_R\big)\Big\}, \end{aligned} \tag{8}$$

in which q_L and q_R denote vectors of quark mass eigenstates in flavor space, $S(\bar{q}_i, q_j; \bar{q}'_k, q'_l)$ is a process dependent symmetry factor and $\Delta F = 1$ FCNCs are described by the off-diagonal elements of the matrices (for c_{Q_i} and c_{q_i} close to $-1/2$)

$$\begin{aligned}(\Delta'_Q)_{ij} \sim (\Delta_Q)_{ij} \sim \frac{1}{2}\,F(c_{Q_i})F(c_{Q_j})\,, \\ (\Delta'_q)_{ij} \sim (\Delta_q)_{ij} \sim \frac{1}{2}\,F(c_{q_i})F(c_{q_j})\,. \end{aligned} \tag{9}$$

The tensor structures

$$\big(\widetilde{\Delta}_Q\big)_{ij} \otimes \big(\widetilde{\Delta}_q\big)_{kl} \sim (\Delta_Q)_{ij}(\Delta_q)_{kl} \sim \frac{1}{4}\,F(c_{Q_i})F(c_{Q_j})F(c_{q_k})F(c_{q_l}) \tag{10}$$

factorize only to leading order and allow for $\Delta F = 2$ FCNCs. Note that order one factors arising from the rotation matrices in (4) are neglected here (see Refs. [4, 5, 7] for details). Using these expressions and Eq. (5), we find that the contributions of the photon KK modes to the Wilson coefficient of the operator

$$\mathcal{O}_{LR} = (\bar{d}_L\gamma_\mu s_L)\,(\bar{d}_R\gamma^\mu s_R) \tag{11}$$

scale parametrically like

$$C_{LR} \sim \frac{\alpha}{M_{\rm KK}^2}\,\frac{m_d m_s}{v^2 Y_*^2}\,. \tag{12}$$

This RS-GIM suppression is very effective, so that almost all flavor observables do still allow for a new physics scale of $M_{\rm KK} \sim 1$ TeV for most of the parameter space. The only exception in the quark sector is CP-violation in Kaon mixing, measured by ϵ_K [2]. This observable is generally large in new physics models which allow for operators of the type in Eq. (11) which couple left- to right-handed quarks. The strong RS-GIM suppression (12) is partially offset in this observable by a model-independent chiral enhancement of the matrix elements and a sizable contribution from renormalization group running [9–13]. Since this is the sole exception to an otherwise excellent model of flavor, many extensions have been proposed in order to solve this RS flavor problem [14–17].

III. CONSTRAINTS

The parameter points considered in this study are chosen to be in agreement with the electroweak precision parameters S and T, the CP violating quantities ϵ'_K/ϵ_K and ϵ_K, as well as with the measurements of the $Z\bar{b}_L b_L$ couplings. The corrections to oblique parameters from KK gauge boson mixing lead to bounds which are independent of the localization or representation of the fermion fields $F(c)$ and the Yukawa couplings Y_*. The requirement to agree with

electroweak precision tests [18] at the three sigma level together with the measured Higgs mass at 126 GeV therefore induces a definite lower bound on the KK scale of

$$M_{\rm KK}^{\rm min} \gtrsim 5\,{\rm TeV}\,, \qquad M_{\rm KK}^{\rm cust} \gtrsim 2\,{\rm TeV}\,, \tag{13}$$

in the minimal and custodial models, respectively. The CP-violating quantities ϵ_K and ϵ'_K/ϵ_K will single out parameter points with an accidentally small phase. Corrections to the $Z\bar{b}_L b_L$ vertex in the minimal model are directly proportional to $1/F^2(c_{u_3})$ and the corresponding constraint will therefore prefer parameter points with a more IR localized right-handed top quark.

In addition to the tree-level observables discussed here, there are flavor-changing processes like $b \to s\gamma$, which only arise at loop-level. Similarly there are loop-level diagrams which can considerably enhance the bounds from ϵ'_K/ϵ_K. Such contributions grow with the Yukawa couplings, while the tree-level effects are $1/Y_*^2$ suppressed [2]. At very large Yukawa couplings these effects can become more important than the tree-level constraints. Moreover, non-perturbativity can become an issue for large Y_*. We will therefore employ an upper bound of $Y_* < 3$, and thus constrain the discussion to models with dominant leading order effects [19].

IV. FUTURE MEASUREMENTS OF QUARK FLAVOR OBSERVABLES

The next generation of flavor measurements will play an important role in determining the possible impact of new physics and given the null results of the first LHC run, it remains that these measurements will show the first signs of interactions beyond the SM. We will concentrate on FCNCs involving down-type quarks in this paper. After the LHC shutdown, NA62 will start its first run in October 2014 and plans to measure the branching fraction $\mathcal{B}(K^+ \to \pi^+\nu\bar{\nu})$ with 10% accuracy [20]. The stopped Kaon experiment ORKA at Fermilab will succeed the BNL experiments E787/949 and aims at 1000 events in this channel, improving the projected NA62 limits by 50%, surpassing the current theory uncertainty. The neutral mode $\mathcal{B}(K_L^0 \to \pi^0\nu\bar{\nu})$ is expected to be discovered at KOTO, the successor of the E391a experiment at KEK, by 2017, with a long-term goal of observing 100 events at the SM rate [21]. Project X, the accelerator project driving the suite of high luminosity experiments at Fermilab, has the potential to substantially improve both these measurements, reaching the few per-cent accuracy level, and to measure the charged lepton channels $\mathcal{B}(K_L^0 \to \ell^+\ell^-)$ for the first time [22]

The upgrade of the B factory in Japan, Super-KEKB, will host Belle II, which will improve many measurements, especially for inclusive processes such as $b \to s\ell^+\ell^-$ [23]. Future B flavor measurements will also be performed at the LHC, where the LHCb upgrade has the potential to follow up on the discovery of the $B_s^0 \to \mu^+\mu^-$ decay [24] by the discovery of the corresponding B^0 decay.

A. $K^+ \to \pi^+\nu\bar{\nu}$ and $K_L^0 \to \pi^0\nu\bar{\nu}$

The theoretically very clean neutral leptonic decays of the K^+ and the K_L^0 are sensitive to new physics effects in $s \to d\nu\bar{\nu}$ transitions, which in the models considered here are only mediated by the exchange of the Z and its KK excitations[2],

$$\mathcal{H}_{\rm eff}^{s\to d\nu\bar{\nu}} = C_\nu^a\,(\bar{d}_L\gamma^\mu s_L)\sum_l(\bar{\nu}_{lL}\gamma_\mu\nu_{lL}) + \tilde{C}_\nu^a\,(\bar{d}_R\gamma^\mu s_R)\sum_l(\bar{\nu}_{lL}\gamma_\mu\nu_{lL})\,, \tag{14}$$

with Wilson coefficients

$$\begin{aligned} C_\nu^{\rm min} &\sim \frac{\pi\alpha}{s_w^2c_w^2\,M_{\rm KK}^2}\Big[L\left(\frac{1}{2}-\frac{s_w^2}{3}\right)+\frac{v^2Y_*^2}{2m_Z^2}\Big]F(c_{Q_1})F(c_{Q_2})\,,\\ \tilde{C}_\nu^{\rm min} &\sim -\frac{\pi\alpha}{s_w^2c_w^2\,M_{\rm KK}^2}\Big[L\frac{s_w^2}{3}+\frac{v^2Y_*^2}{2m_Z^2}\Big]F(c_{d_1})F(c_{d_2})\,, \end{aligned} \tag{15}$$

in the minimal model and

$$\begin{aligned} C_\nu^{\rm cust} &\sim -\frac{\pi\alpha}{s_w^2c_w^2\,M_{\rm KK}^2}\,\frac{v^2Y_*^2}{2m_Z^2}\,F(c_{d_1})^2F(c_{Q_1})F(c_{Q_2})\,,\\ \tilde{C}_\nu^{\rm cust} &\sim -\frac{\pi\alpha}{s_w^2c_w^2\,M_{\rm KK}^2}\Big[L\,c_w^2+\frac{v^2Y_*^2}{2m_Z^2}\Big]F(c_{d_1})F(c_{d_2})\,, \end{aligned} \tag{16}$$

[2] Scalar contributions are tiny because of the negligible neutrino masses.

in the custodially protected model.[3] Note that each term in the Wilson coefficients above comes with a different phase factor, which is a function of the Yukawa couplings and has been omitted for simplicity. The terms proportional to Y_* represent contributions from the mixing of the fermions with their KK modes, which can become important for large $Y_* > 1$. The mixing of the Z with its excitations generates the contributions which are not directly proportional to Y_*. Rewriting the expressions (15) and (16) in terms of the free RS-flavor parameters Y_* and $F(c_{u_3})$, we can see that in the minimal model the left-handed quark currents are generically subject to the largest corrections. Given $Y_* \lesssim 1$, these corrections scale to good approximation like $C_\nu^{\rm min} \sim Y_*^{-2} F(c_{u_3})^{-2}$. Note that only for large $Y_* \sim Y_*^{\rm max} \sim 3$ and a strongly IR localized top quark, $F(c_{u_3}) > 1$ can the corrections to the right handed currents become dominant: these then scale like $\tilde{C}_\nu^{\rm min} \sim Y_*^2 F(c_{u_3})^2$.

In the custodial model, fermion mixing entering the left-handed currents is always suppressed by m_d^2/m_Z^2 and the contributions of the neutral gauge bosons to these currents cancel, so that basically only contributions to the right-handed currents remain.

We define $X \equiv 1.24\, e^{2.87\, i} + X_{\rm RS}^a$, in which

$$X_{\rm RS}^a = \frac{s_w^4 c_w^2 m_Z^2}{\alpha^2 \lambda^5} \left(C_\nu^a + \tilde{C}_\nu^a \right), \tag{17}$$

and $a = \min$ or $a = \text{cust}$. Therefore we can write

$$\mathcal{B}(K_L \to \pi^0 \nu\bar{\nu}) = \kappa_L \left(\text{Im}\, X \right)^2, \tag{18}$$

$$\mathcal{B}(K^+ \to \pi^+ \nu\bar{\nu}(\gamma)) = \kappa_+ \left(1 + \Delta_{\rm EM}\right) \left| X \right|^2, \tag{19}$$

in which κ_+, κ_L and $\Delta_{\rm EM}$ are given in Appendix A. As discussed above, the contributions from the Z and its KK modes as well as from additional neutral KK modes from the extended gauge group lead generically to opposite chiral structures in the minimal and custodial model. Both observables (18) and (19), however, cannot resolve this structure and therefore cannot unambiguously distinguish between the two models. For negligible effects from fermion mixing, the contributions in the minimal model compared to the custodial model scale like

$$\frac{X_{\rm RS}^{\rm min}}{X_{\rm RS}^{\rm cust}} \sim \frac{1}{2} \frac{F(c_{Q_1}) F(c_{Q_2})}{F(c_{d_1}) F(c_{d_2})} = \lambda^{10} A^4 \frac{m_t^4}{v^2\, m_d\, m_s} \frac{1}{Y_*^2} \frac{1}{F(c_{u_3})^4} \approx \frac{6}{Y_*^2 F(c_{u_3})^4}\,. \tag{20}$$

This leads to generically larger effects in the minimal model. The scatter plots in Figure 1, which scan the parameter space in the allowed $M_{\rm KK}$ range, assuming Yukawa couplings with $Y_* = 1$ and $(Y_q)_{ij} < 3$, illustrate this result (recall that the mass scale for parameter points allowed by electroweak constraints is smaller in the custodial model by roughly a factor of two, which partially cancels this effect).

From (20), it is clear, that an IR shift of the right-handed profiles into the ($c_{t_R} \equiv c_{u_3} \gtrsim 1$) region leads to an enhanced (decreased) effect in the custodial (minimal) model and similarly a UV shift ($c_{t_R} < 0.2$) would have the opposite effect. This behaviour is illustrated in Figure 2.

The large errors on the current experimental value $\mathcal{B}(K^+ \to \pi^+ \nu\bar{\nu})_{\rm exp} = 1.73^{+1.15}_{-1.05} \times 10^{-10}$ accommodate both models [26]. We want to emphasize that a future measurement with 10% precision could help to draw a much clearer picture. If new measurements point to larger values compared to the SM, the custodially protected RS model will be pushed to extreme corners of the parameter space[4]. Constraints from ϵ'_K/ϵ_K suppress effects in $\mathcal{B}(K_L^0 \to \pi^0 \nu\bar{\nu})$ in both models (see [5] for details). A non-SM measurement of this ultra-rare decay would therefore pose a challenge for RS type models.

B. $K_L^0 \to \mu^+\mu^-$

Contributions to decays into charged leptons are generated through exchange of the Z, its excitations and photon KK modes in the considered models. There are additional scalar contributions, which we neglect because they are suppressed by the masses of the light leptons. We therefore find

$$\mathcal{H}_{\rm eff}^{s \to d l^+ l^-} = C_{l1}^a \left(\bar{d}_L \gamma^\mu s_L\right) \sum_l \left(\bar{l}_L \gamma_\mu l_L\right) + C_{l2}^a \left(\bar{d}_L \gamma^\mu s_L\right) \sum_l \left(\bar{l}_R \gamma_\mu l_R\right) \tag{21}$$

$$+ \tilde{C}_{l1}^a \left(\bar{d}_R \gamma^\mu s_R\right) \sum_l \left(\bar{l}_R \gamma_\mu l_R\right) + \tilde{C}_{l2}^a \left(\bar{d}_R \gamma^\mu s_R\right) \sum_l \left(\bar{l}_L \gamma_\mu l_L\right) \tag{22}$$

---

[3] See Refs. [5, 7, 25] for a discussion of the changes that appear for the custodial model.

[4] It should be specified, that models with different fermion representations could accommodate such an effect [27].

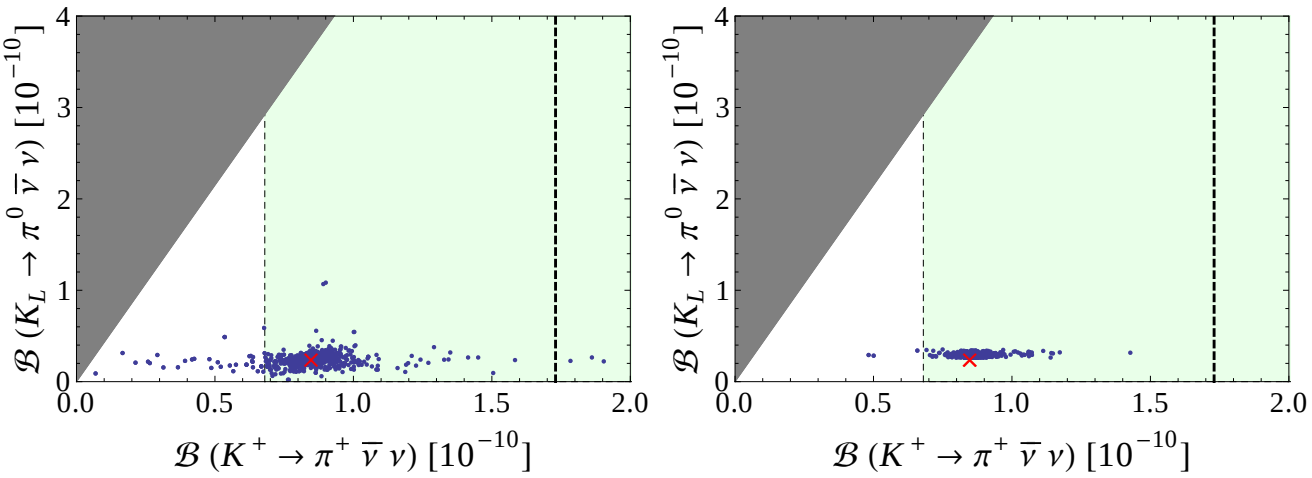

FIG. 1: Scatter points in the $\mathcal{B}(K_L \to \pi^0 \nu\bar{\nu}) - \mathcal{B}(K^+ \to \pi^+ \nu\bar{\nu})$ plane for the minimal (custodial) model on the left (right) panel. The SM prediction is shown as a red cross. The dark gray region is theoretically excluded (Grossmann-Nir bound) and the experimentally preferred region is shown in light blue.

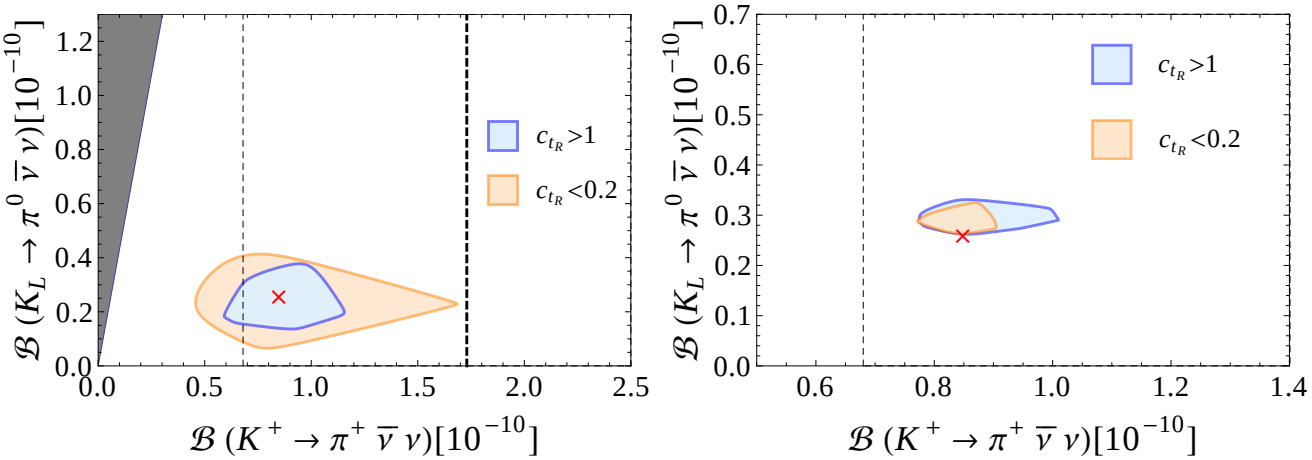

FIG. 2: Regions covering the parameter points between the 2.5% and 97.5% quantile in Fig. 1. Blue (orange) regions represent 95% of models with strongly (less strong) IR-localized right-handed tops. The SM prediction is shown as a red cross. The dark gray region is theoretically excluded (Grossmann-Nir bound) and the central value and the one-sided one sigma limit of the experimental value is shown by dashed lines. The left (right) panel show the size of possible effects in the minimal (custodial) model.

with the following coefficients in the minimal model,

$$
\begin{aligned}
C_{l1}^{\rm min} &= -\Big[\frac{2\pi\alpha}{3M_{\rm KK}^2} + \frac{\pi\alpha\,(1-2s_w^2)}{s_w^2 c_w^2\,M_{\rm KK}^2}\left\{L\left(\frac{1}{2}-\frac{s_w^2}{3}\right)+\frac{v^2Y_*^2}{2m_Z^2}\right\}\Big]\,F(c_{Q_1})F(c_{Q_2})\,,\\
\tilde{C}_{l1}^{\rm min} &= -\Big[\frac{2\pi\alpha}{3M_{\rm KK}^2} + \frac{2\pi\alpha}{c_w^2\,M_{\rm KK}^2}\left\{L\,\frac{s_w^2}{3}+\frac{v^2Y_*^2}{2m_Z^2}\right\}\Big]\,F(c_{d_1})F(c_{d_2})\,,\\
C_{l2}^{\rm min} &= -\Big[\frac{2\pi\alpha}{3M_{\rm KK}^2} - \frac{2\pi\alpha}{c_w^2\,M_{\rm KK}^2}\left\{L\left(\frac{1}{2}-\frac{s_w^2}{3}\right)+\frac{v^2Y_*^2}{2m_Z^2}\right\}\Big]\,F(c_{Q_1})F(c_{Q_2})\,,\\
\tilde{C}_{l2}^{\rm min} &= -\Big[\frac{2\pi\alpha}{3M_{\rm KK}^2} - \frac{\pi\alpha\,(1-2s_w^2)}{s_w^2 c_w^2\,M_{\rm KK}^2}\left\{L\,\frac{s_w^2}{3}+\frac{v^2Y_*^2}{2m_Z^2}\right\}\Big]\,F(c_{d_1})F(c_{d_2})\,,
\end{aligned}
\tag{23}
$$

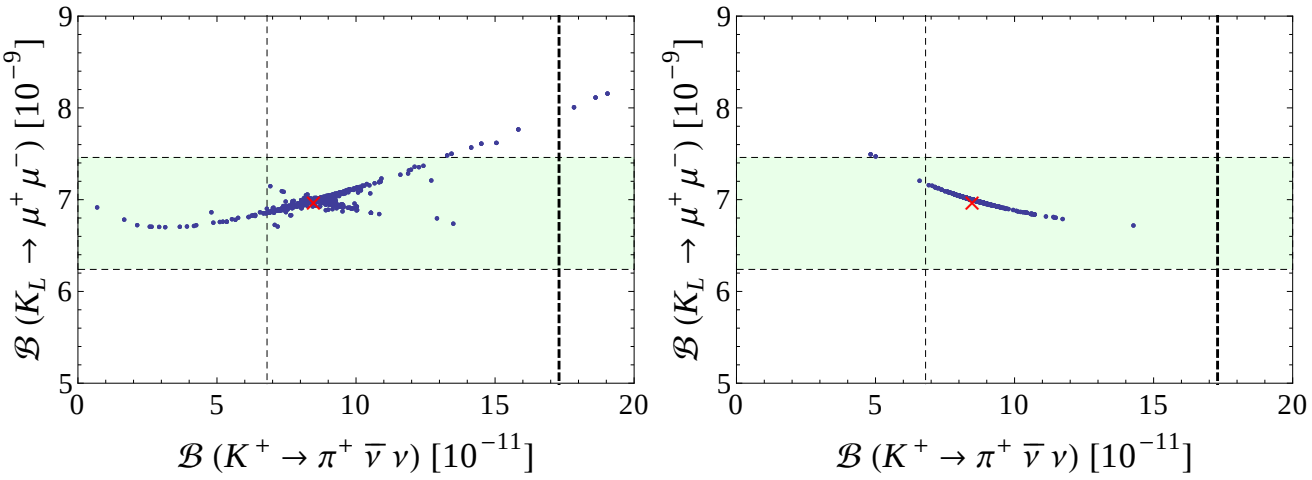

FIG. 3: Scatter points in the $\mathcal{B}(K_L \to \mu^+\mu^-) - \mathcal{B}(K^+ \to \pi^+\nu\bar{\nu})$ plane for the minimal (custodial) model on the left (right) panel. The SM prediction is shown as a red cross. A one sigma band combining experimental and theoretical errors for $\mathcal{B}(K_L \to \mu^+\mu^-)$ is shown in light blue. The central value (and the one-sided one sigma limit) for $\mathcal{B}(K^+ \to \pi^+\nu\bar{\nu})$ is shown as a thick (thin) dashed line.

and in the case of the custodially protected model

$$
\begin{aligned}
C_{l1}^{\rm cust} &= -\Big[\frac{2\pi\alpha}{3M_{\rm KK}^2} - \frac{\pi\alpha\,(1-2s_w^2)}{s_w^2 c_w^2\,M_{\rm KK}^2}\frac{v^2Y_*^2}{2m_Z^2}F(c_{d_1})^2\Big]\,F(c_{Q_1})F(c_{Q_2})\,,\\
\tilde{C}_{l1}^{\rm cust} &= -\Big[\frac{2\pi\alpha}{3M_{\rm KK}^2} + \frac{2\pi\alpha}{M_{\rm KK}^2}\left\{L + \frac{v^2Y_*^2}{2c_w^2 m_Z^2}\right\}\Big]\,F(c_{d_1})F(c_{d_2})\,,\\
C_{l2}^{\rm cust} &= -\Big[\frac{2\pi\alpha}{3M_{\rm KK}^2} + \frac{2\pi\alpha}{M_{\rm KK}^2}\frac{v^2Y_*^2}{2c_w^2 m_Z^2}F(c_{d_1})^2\Big]\,F(c_{Q_1})F(c_{Q_2})\,,\\
\tilde{C}_{l2}^{\rm cust} &= -\Big[\frac{2\pi\alpha}{3M_{\rm KK}^2} - \frac{\pi\alpha\,(1-2s_w^2)}{s_w^2\,M_{\rm KK}^2}\left\{L + \frac{v^2Y_*^2}{2c_w^2 m_Z^2}\right\}\Big]\,F(c_{d_1})F(c_{d_2})\,.
\end{aligned}
\tag{24}
$$

In both models the first term of each Wilson coefficient is the same and corresponds to the contribution from the KK photon exchange. In the custodially protected model, the contributions to the left-handed quark-currents from the Z and its excitations cancel again with the KK excitations of the additional heavy neutral $SU(2)_R$ gauge bosons, while the fermion mixing terms are suppressed by m_d^2/m_Z^2.

Taking into account low energy contributions, the branching ratio of the $K_L \to \mu^+\mu^-$ decay can be written as [31]

$$
\mathcal{B}(K_L \to \mu^+\mu^-) = \Big(6.7 + \big[1.1\,\mathrm{Re}\,Y_A' - 0.55\big]^2\Big)\cdot 10^{-9}\,. \tag{25}
$$

It is only sensitive to the axial vector currents

$$
Y_A' = \frac{s_w^2 c_w^2 m_Z^2}{2\pi\alpha^2\lambda_t^{(ds)}}\left(C_{l1}^a - C_{l2}^a + \tilde{C}_{l1}^a - \tilde{C}_{l2}^a\right)\,, \tag{26}
$$

for $a = $ min or $a =$cust. Therefore, the contributions from photon KK modes cancel in both models. Since $C_{l1}^a - C_{l2}^a = -C_\nu^a$ and $\tilde{C}_{l1}^a - \tilde{C}_{l2}^a = \tilde{C}_\nu^a$, similar to the discussion in the last subsection, in the minimal model the left-handed currents dominate for most of the parameter space, while the custodial protection allows only for the right-handed currents to contribute to $\mathcal{B}(K_L \to \mu^+\mu^-)$.

Figure 3 shows scatter plots in the $\mathcal{B}(K_L \to \mu^+\mu^-) - \mathcal{B}(K^+ \to \pi^+\bar{\nu}\nu)$ plane for the minimal (left panel) and custodially protected model (right panel). The expected correlations for new physics with dominant left- (right-) handed flavor-changing currents are clearly visible in the left (right) panel [5, 27]. In the light of a precise future measurement of $K^+ \to \pi^+\bar{\nu}\nu$ and similar progress in the theoretical determination of the long-distance contributions to $K_L \to \mu^+\mu^-$ can therefore clearly distinguish between the models considered here. The possible size of effects depends again on the localization of the right handed top quark and folows a similar pattern as in Figure 2. As in Section (IV A), this can be understood in the parametric dependence of the ratio of left- and right-handed profiles,

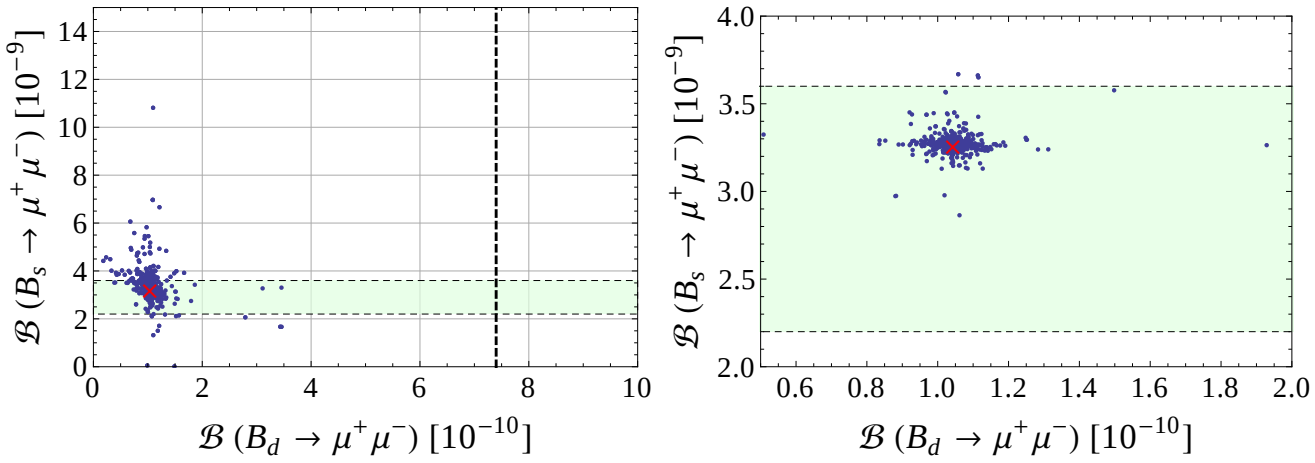

FIG. 4: Scatter points in the $\mathcal{B}(B_d \to \mu^+\mu^-) - \mathcal{B}(B_s \to \mu^+\mu^-)$ plane for the minimal (custodial) model on the left (right) panel. The SM prediction is shown as a red cross. A one sigma band for the experimental value of $\mathcal{B}(B_s \to \mu^+\mu^-)$ is shown in light blue. The upper limit for $\mathcal{B}(B_d \to \mu^+\mu^-)$ is shown as a dashed line.

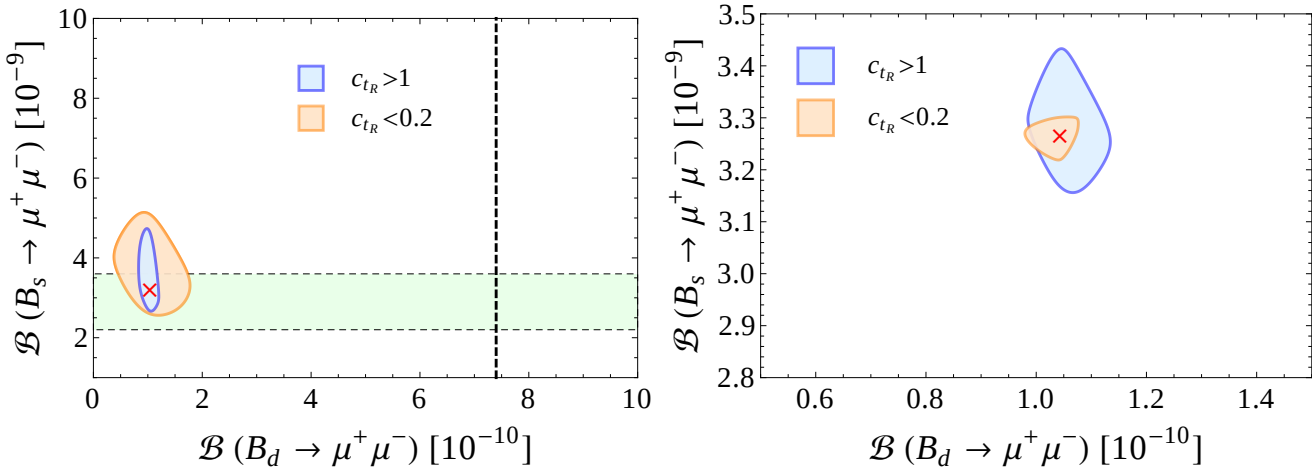

FIG. 5: Regions covering the parameter points between the 2.5% and 97.5% quantile in Fig. 5. Blue (orange) regions represent 95% of models with strongly (less strong) IR-localized right-handed tops. The SM prediction is shown as a red cross The one sigma band of the experimental value for $\mathcal{B}(B_s \to \mu^+\mu^-)$ and the upper limit on $\mathcal{B}(B_d \to \mu^+\mu^-)$ are shown by dashed lines. The left (right) panel show the size of possible effects in the minimal (custodial) model.

which control the size of effects in the Wilson coefficients (23) and (24).[5]

C. $B_{s,d} \to \mu^+\mu^-$

The branching ratios for the $B_q \to \mu^+\mu^-$ decays can be expressed as

$$\mathcal{B}(B_q \to \mu^+\mu^-) = \frac{G_F^2\,\alpha^2\,m_{B_q}^3 f_{B_q}^2 \tau_{B_q}}{64\pi^3 s_w^4} \left|\lambda_t^{(qb)}\right|^2 \sqrt{1-\frac{4m_\mu^2}{m_{B_q}^2}}\,\frac{4m_\mu^2}{m_{B_q}^2}\,\left|c_A + C^a\right|^2, \tag{27}$$

where m_{B_q}, f_{B_q}, and τ_{B_q} denote the mass, decay constant, and lifetime of the B_q meson (numerical values are collected in Appendix A) and $c_A = 0.96 \pm 0.02$ is the SM contribution [32, 33]. Again, scalar contributions are not explicitly

[5] The strong correlation between the two observables would lead to a misrepresentation of the data in a two-dimensional fit based on the convex hull. Therefore we do not present an illustration of this parametrical dependence.

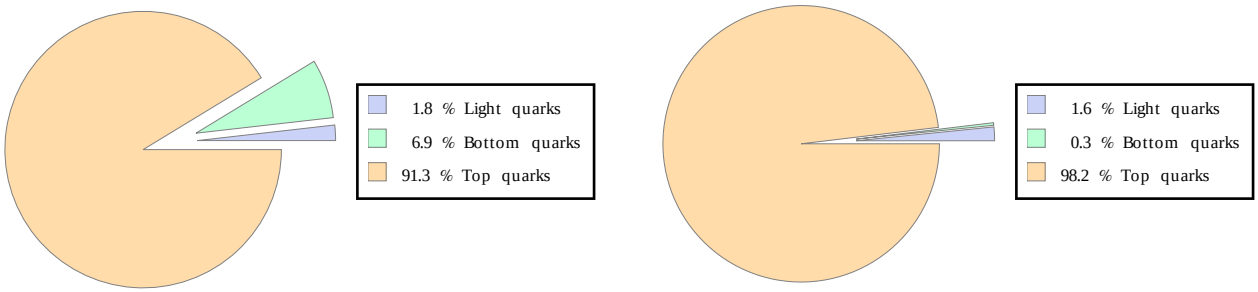

FIG. 6: Pie charts of the branching fractions of the first KK gluon into light quarks, bottom quarks and top quarks in the minimal model. The left chart shows the mean values of our parameter points with $c_{u_3} < 0.2$, while the right chart displays the mean values of our parameter points with $c_{u_3} > 1.5$.

given, because they are additionally suppressed by light masses. The RS contribution reads

$$C_q^a = -\frac{s_w^4 c_w^2 m_Z^2}{\alpha^2 \lambda_t^{(qb)}} \left(C_{l1}^a - C_{l2}^a + \tilde{C}_{l1}^a - \tilde{C}_{l2}^a \right). \tag{28}$$

The Wilson coefficients follow from (23) for a =min, and from (24) for a =cust, with the replacements $F(c_{Q_1})F(c_{Q_2}) \to F(c_{Q_1})F(c_{Q_3})$ and $F(c_{d_1})F(c_{d_2}) \to F(c_{d_1})F(c_{d_3})$ for $B_d \to \mu^+\mu^-$. In the case of $B_s \to \mu^+\mu^-$, we replace $F(c_{Q_1})F(c_{Q_2}) \to F(c_{Q_2})F(c_{Q_3})$ and $F(c_{d_1})F(c_{d_2}) \to F(c_{d_2})F(c_{d_3})$, as well as the suppression of the fermion mixing terms in the custodial scenario, for which $F(c_{d_1})^2 \to F(c_{d_2})^2$. Contributions from KK photon exchange cancel again in both models. In contrast to Kaon decays, however, the ratio of left- to right-handed couplings in the decays of B_q mesons is enhanced by roughly an order of magnitude in the minimal model, which is reflected in (again neglecting contributions from fermion mixing)

$$\frac{C_q^{\min}}{C_q^{\text{cust}}} \approx \frac{1}{2} \frac{F(c_{Q_3})F(c_{Q_i})}{F(c_{d_3})F(c_{d_i})} = \lambda^{8-2i} A^2 \frac{m_t^4}{v^2 m_b m_{d_i}} \frac{1}{Y_*^2} \frac{1}{F(c_{u_3})^4} \approx \frac{100}{Y_*^2 F(c_{u_3})^4}, \tag{29}$$

with $i = 1$ for B_d decays and $i = 2$ in the case of B_s decays, and the last expression is valid in both cases approximately. As a consequence, effects in the custodially protected model turn out to be even smaller compared to the minimal model, as displayed by the scatter plots in Figure 4. The opposite scaling behaviour with c_{u_3} of effects in the minimal and custodial model is shown by plots with fits to all parameter points in between the 2.5% and 97.5% quantiles for strongly and less strong IR localized top quarks in Figure 5. The upgraded LHCb is expected to measure $\mathcal{B}(B_s \to \mu^+\mu^-)$ with 8% accuracy and to detect enough events in order to measure $\mathcal{B}(B_d \to \mu^+\mu^-)/\mathcal{B}(B_s \to \mu^+\mu^-)$ with 35% accuracy, given it is SM like. Both these measurements will cut into the parameter space of the models considered here, even for the high masses of the new resonances expected from electroweak precision tests.

V. FLAVOR VS COLLIDER OBSERVABLES

At leading order, a single KK gluon resonance cannot be produced from gluon initial states. The production at the LHC is therefore suppressed by the quark-anti-quark parton density functions (PDFs) at $\sqrt{s} = 14$ TeV. The couplings of a KK gluon to quarks is also flavor-dependent and can be described by the same wavefunction overlap integrals which appear in equation (8). The coupling of the first gluon KK mode to quarks can be written as

$$g_s \left(g_L^{1ij}\, \bar{q}_i\, \gamma_\mu T^A G_A^\mu\, P_L\, q_j + g_R^{1ij}\, \bar{q}_i\, \gamma_\mu T^A\, G_A^\mu P_R\, q_j \right), \tag{30}$$

with i, j flavor indices, G_A^μ the gluon KK mode and T^A the $SU(3)$ generators. For the coupling we find

$$g_X^{1ij} \approx \frac{m_{G^1}}{\sqrt{2} M_{\text{KK}}} \left(\frac{1}{\sqrt{2L}}\, \delta_{ij} - \sqrt{2L}\, (\Delta')_{ij} \right) \tag{31}$$

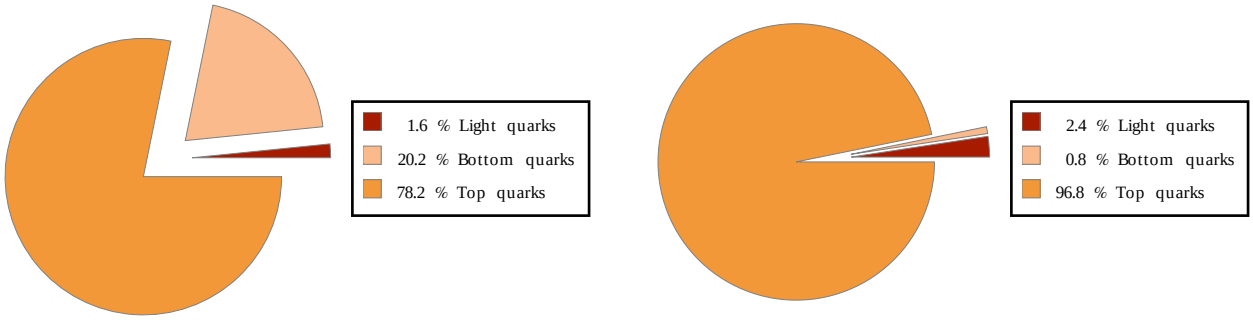

FIG. 7: Pie charts of the branching fractions of the first KK gluon into light quarks, bottom quarks and top quarks in the custodial model. The left chart shows the mean values of our parameter points with $c_{u_3} < 0.2$, while the right chart displays the mean values of our parameter points with $c_{u_3} > 1.5$.

in which $m_{G^1} \approx 2.4\, M_{\rm KK}$ is fixed by the boundary conditions of the 5D gluon and $\Delta' \sim F(c_{Q_i})F(c_{Q_j})$ for $X = L$ and $\Delta' \sim F(c_{q_i})F(c_{q_j})$ for $X = R$. [6] For flavor-diagonal couplings this results in the parametric dependence

$$F(c_{Q_i})^2 = \frac{2m_t^2}{v^2 Y_*^2}\,\frac{1}{F(c_{u_3})^2} \times \begin{cases} \lambda^6 A^2\,, & \text{for} \quad i = 1 \\ \lambda^4 A^2\,, & \text{for} \quad i = 2 \\ 1\,, & \text{for} \quad i = 3 \end{cases}, \tag{32}$$

$$F(c_{q_i})^2 = \frac{m_{q_i}^2}{m_t^2} F(c_{u_3})^2 \times \begin{cases} \lambda^{-6} A^{-2}\,, & \text{for} \quad q_i = u, d \\ \lambda^{-4} A^{-2}\,, & \text{for} \quad q_i = c, s \\ 1\,, & \text{for} \quad q_i = b, t \end{cases}. \tag{33}$$

For light quarks, Eq. (31) is therefore clearly dominated by the universal term, which is absent for flavor off-diagonal couplings. For IR localized profiles, the flavor non-universal part dominates and can enhance the QCD coupling by a factor of a few. In the models considered here, only the coupling to right-handed top quarks can be subject to such an enhancement. In the dual language, this can be interpreted as the result of both the KK gluons and the top quark being mostly composite and therefore strongly feel the composite-composite couplings, whereas the elementary light quarks couple to composites only after mixing with their resonances. As a result, the KK gluon decays dominantly into top quarks. From Eq. (32) it follows that for a UV shifted right-handed top profile, however, the coupling to the third generation electroweak doublet can be enhanced and consequentially the partial decay width of the KK gluon into bottom quarks can become non-negligible. Figures 6 and 7 illustrate the branching fractions of the first KK gluon excitation into light quarks, bottom quarks and top quarks for the minimal and custodial models. The left hand side shows the mean value of the branching fractions of our parameter set for a UV shifted right-handed top profile ($c_{u_3} < 0.2$), while the right-hand side displays the corresponding chart for parameter points with a strongly IR localized right-handed top ($c_{u_3} > 1.5$).

The differences between the minimal and the custodial model are rooted in the constraint from the $Z\bar{b}_L b_L$ coupling, since this coupling increases with a more IR localized third generation electroweak doublet and hence the constraint has a bigger impact in the minimal model. While a direct search for models with $c_{u_3} > 1.5$ is therefore most promising in the $t\bar{t}$ spectrum, the $c_{u_3} < 0.2$ scenario could be probed in dijet searches at an upgraded LHC or a future collider. In the left panel of Figure 8, we show the 95% C.L. exclusion limits possible at 14 TeV, 33 TeV, and 100 TeV pp colliders with 300 fb^{-1} or 3 ab^{-1} of integrated luminosity in the M_G vs. c_{u3} plane in the dijet search channel. These limits are based on the work of [28, 29], and unlike the flavor-universal case in universal extra dimensions [30], the KK gluon mass reach suffers because of the small production cross section and small dijet branching fraction. Interestingly, for the custodial model the sensitivity of dijet searches grows for a parameter region in which the sensitivity of flavor measurements decreases. The right panel of Figure 8 shows that the sensitivity in the $t\bar{t}$ final state only depends weakly on the localization of the right handed top quark c_{u_3}. This is expected, because in the considered parameter region the coupling of the KK gluon to top quarks grows only linearly with c_{u_3}.

[6] Notice that this approximation of the flavor dependent part is again only valid up to order one factors and therefore only captures the parametric dependence of the KK gluon couplings.

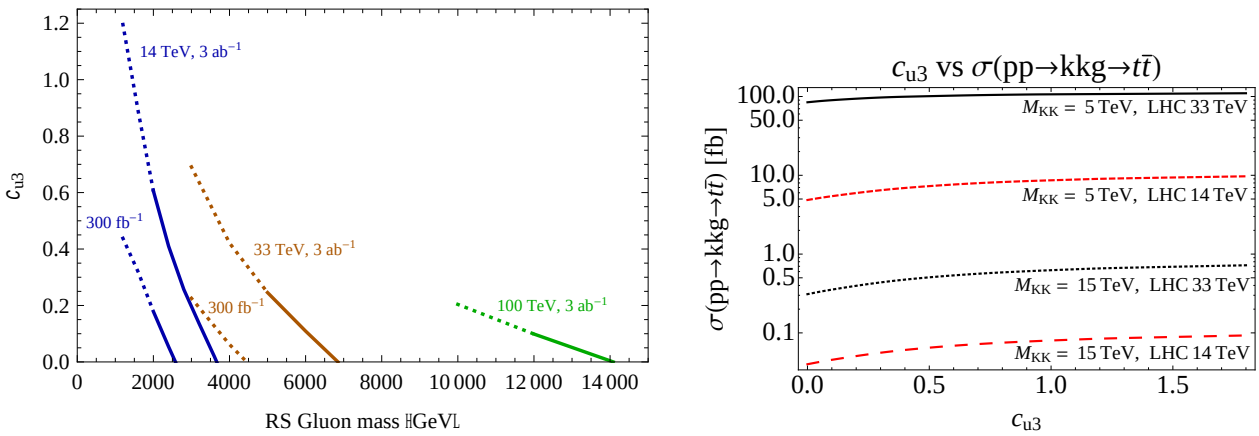

FIG. 8: The left panel shows projected 95% C.L. exclusion contours for 14 TeV (dark blue solid), 33 TeV (dark brown solid), and 100 TeV (dark green solid) in the c_{u_3} versus KK gluon mass plane from dijet resonance searches. The regions below each line are excluded. The dotted lines indicate an extrapolation of the projected exclusion limits to low multijet trigger thresholds. The right panel shows the c_{u_3} dependence of the cross section for the decay of first KK gluon excitation into $t\bar{t}$ pairs.

VI. LEPTON SECTOR: ANARCHIC MODELS

Partial compositeness can account for the mass hierarchy in the charged lepton sector in analogy with the quark sector. The main qualitative differences between the two sectors arise because: (1) the neutrino mass matrix is non-hierarchical, and (2) flavor-changing processes in the charged lepton sector have not been observed.

A. Neutrino masses in anarchic scenarios

We will here show how an anarchic framework can correctly reproduce both the hierarchical charged lepton masses and the non-hierarchical neutrino mass matrix. Other models for neutrino masses employ discrete symmetries (see e.g. [34–36]).

To achieve our goal two different ways have been proposed, depending on whether the neutrinos are Dirac [37] or Majorana [38]. Both mechanisms rely on the presence of new, UV-sensitive sources for the neutrino mass matrix, and in turn require new physics at or below the see-saw scale. If neutrinos are Dirac, the RH neutrinos N will also be allowed to mix with composites of the strong dynamics. Then, up to cutoff suppressed operators, the lepton Yukawas will be parametrized in the IR by terms like $y_\nu \bar{\ell} H N$, with ℓ the lepton doublet and

$$y_\nu \sim Y_* \left(\frac{M_{\rm KK}}{\Lambda_{\rm UV}}\right)^{\Delta_\ell + \Delta_N - 5} . \tag{34}$$

Here Y_* denotes a coupling between the composite states, $\Lambda_{\rm UV}$ is the UV cutoff (assumed to be below the Planck scale), and $\Delta_{\ell,N}$ the scaling dimension of the composites mixing with ℓ, N. The point raised in Ref. [37] is that if Δ_N is sufficiently large, the above Yukawa will become so small that cutoff-suppressed operators might become more important. The lowest dimension cutoff-suppressed operator we can write compatible with lepton number involves the pair $\bar{\ell} N$, but the operator cannot be written using the Higgs doublet because this field is a composite state emergent in the deep IR. Yet, the strong sector necessarily possesses an operator $\mathcal{O}_H$ with the same quantum numbers of H, allowing us to write $\bar{\ell}\mathcal{O}_H N$. This coupling will only receive flavor-universal renormalization effects from the strong dynamics due to the anomalous dimension of $\mathcal{O}_H$, and the neutrino mass matrix will be:

$$y_\nu \sim Y_* \left(\frac{M_{\rm KK}}{\Lambda_{\rm UV}}\right)^{\Delta_H - 1} . \tag{35}$$

The matrix Y_* is non-hierarchical if the physics above the cutoff $\Lambda_{\rm UV}$ is generic, and this translates into non-hierarchical neutrino masses. In a large N theory the absence of UV sensitivity of the "mass operator" $\mathcal{O}_H^\dagger \mathcal{O}_H$ demands $\Delta_H \geq 2$, and to get $m_\nu = O(0.05)$ eV with $Y_* \lesssim 4\pi$ we need $\Lambda_{\rm UV} \lesssim 10^{13-14} M_{\rm KK}$.

In Ref. [38] it has been emphasized that cutoff-suppressed operators are always important if neutrinos are Majorana. In this case N is not there, and the leading operator contributing to neutrino masses is $\overline{\ell^c}\tau^a \ell \mathcal{O}_T^a$, with $\mathcal{O}_T$ the most

relevant electroweak triplet, Lorentz scalar we can construct with the fields of the strong sector. In the IR this results in

$$y_\nu \propto \left(\frac{M_{\rm KK}}{\Lambda_{\rm UV}}\right)^{\Delta_T-1}. \tag{36}$$

and typically requires a cutoff scale $\Lambda_{\rm UV}$ comparable to the Dirac neutrino case. Similarly to the previous case, the neutrino masses will be anarchic if the physics at the cutoff has no flavor structure.

There are two qualitative differences between these two scenarios. Perhaps the most trivial one is that in this latter model the neutrinos are Majorana, and therefore predicts neutrino-less $\beta\beta$ decay and the standard phenomenology for Majorana neutrinos.

At a more technical level, we find that the two models have different TeV scale phenomenology when realized in minimal 5D scenarios. In particular, the Majorana neutrino scenario of [38] requires the introduction of additional bulk scalars. Indeed, while from the 4D point of view the existence of an electroweak triplet composite operator is a generic expectation in strongly coupled theories, in minimal 5D realizations a field with the required properties is not necessarily present. A bulk Higgs pair $H^\dagger\tau^a H$ would not do the job because its overlap with the UV brane (where the leptons are peaked) is too small: in that case $\Delta_T = 2\Delta_H \gtrsim 4$, and in order to generate a m_ν of the correct order of magnitude $\Lambda_{\rm UV}$ would be required to be unacceptably low.

The most minimal 5D realization of the scenario envisioned in Ref. [38] includes a bulk scalar triplet T^a with hypercharge 1, a 4D mass $m_T \sim M_{\rm KK}$, a coupling $\overline{\ell^c}\tau^a\ell T^a$, and a vertex $\lambda_T M_{\rm KK}\tilde{H}^\dagger\tau^a H T^a$. Once the scalar is integrated out we get

$$\begin{aligned} m_\nu &= Y_T\left(\frac{m_T}{\Lambda_{\rm UV}}\right)^{\Delta_T-1}\frac{\lambda_T M_{\rm KK}}{m_T^2}v^2 \\ &\sim Y_T\left(\frac{m_T}{\Lambda_{\rm UV}}\right)^{\Delta_T-2}\lambda_T\frac{v^2}{\Lambda_{\rm UV}}, \end{aligned} \tag{37}$$

where the flavor-universal factor $\sim (M_{\rm KK}/\Lambda_{\rm UV})^{\Delta_T-1}$ results from warping the coupling to leptons down to the TeV scale. For a 5D mass close to saturating the bound $\Delta_T \sim 2$, we need $\Lambda_{\rm UV} \lesssim \lambda_T \times 10^{16}$ GeV to get $m_\nu = O(0.05)$ eV.

Two more points are worth stressing. First, after electroweak symmetry breaking, the trilinear λ_T leads to a tadpole diagram which results in a vacuum expectation value (vev) $v_T = \lambda_T M_{\rm KK} v^2/m_T^2$ for the neutral component of T. This in turn contributes to the ρ parameter, or equivalently:

$$\alpha_{\rm em}\Delta T = -4\frac{v_T^2}{v^2} = -4\left(\frac{\lambda_T M_{\rm KK} v}{m_T^2}\right)^2. \tag{38}$$

Taking for definiteness $m_T = M_{\rm KK}$, we find that the bound $|\alpha_{\rm em}T| \lesssim 10^{-3}$ is easily satisfied in models where $M_{\rm KK}$ is above a few TeV even for $\lambda_T = O(1)$. This coupling can be naturally small because it carries custodial $SU(2)$ spurionic quantum numbers, but cannot be arbitrarily small if we want to keep $\Lambda_{\rm UV}$ safely above the TeV scale. The regime $m_T \ll M_{\rm KK}$ is clearly disfavored, and suggests that the collider signatures of the triplet might well be suppressed in a realistic model.

We also note that the presence of a vev for the triplet does not lead to an anomalously light Majoron, the would-be Goldstone boson associated with the breaking of the lepton number. This is because the very same coupling λ_T that controls spontaneous breaking of $U(1)_L$ also controls the explicit breaking. Indeed, for $\lambda_T = 0$ the model has an unbroken (and typically anomalous) global $U(1)_L$ and a degenerate triplet with mass m_T. As soon as λ_T is switched on, the global symmetry is explicitly broken, and by continuity we expect the triplet masses squared to be $\sim m_T^2$ up to a splitting of $O(\lambda_T)$. [7]

It is important to appreciate that the physics of the charged leptons is essentially unaffected by the mechanism invoked to generate the neutrinos masses. We therefore conclude that the charged lepton observables as well as the collider phenomenology of the two realizations [37, 38] are basically the same.

---

[7] To rigorously show that the CP-odd scalar π in $T^{(0)} = (v_T + \delta T)e^{i\pi/v_T}$ is not a light Majoron with "decay constant" v_T we can employ the standard formula for the mass of a Goldstone mode in the presence of an anomalous current, $m_\pi^2 \approx -\langle 0|\mathcal{A}|\pi\rangle/f_\pi$. Then, specializing to our case, the anomaly reads $\mathcal{A} \equiv \partial_\mu J^\mu_{U(1)_L} = +i\lambda_T M_{\rm KK}\tilde{H}^\dagger\tau^a H T^a + \text{h.c.} = -v_T m_T^2\pi + \dots$ and the decay constant is $f_\pi = v_T$, so one finds $m_\pi^2 \approx m_T^2$ as anticipated by the continuity argument.

VII. LEPTON FLAVOR OBSERVABLES IN THE ANARCHIC SCENARIO

We now discuss the lepton observables that are most sensitive to the new physics scale of anarchic scenarios. The literature devoted to a systematic study of this subject is quite modest compared to the number of works on the quark sector, see for example [38–40]. Below we summarize the main current and projected bounds.

Observable	SM Theory	Current Expt.	Future Experiments
a_μ	$\Delta a_\mu = (287 \pm 80) \times 10^{-11}$ (E821)		error/4 E989
$\lvert d_\mu \rvert$	$< 10^{-38}$	$< 1.9 \times 10^{-19}$ecm (E821)	$< 10^{-21}$ E989
$\mathcal{B}(\mu^+ \to e^+\gamma)$	$\sim 10^{-52}$	$< 5.7 \times 10^{-13}$ MEG [47]	$< 10^{-14}$ MEG[48]
$\mathcal{B}(\mu \to 3e)$	$\ll 10^{-52}$	$< 1 \times 10^{-12}$ SINDRUM	$< 10^{-16}$ Mu3e [49]
$R_{\mu e} = \frac{\mathcal{B}(\mu A(Z,N) \to e A(Z,N))}{\mathcal{B}(\mu A(Z,N) \to \nu_\mu A(Z-1,N))}$	$\ll 10^{-52}$	$< 7 \times 10^{-13}$ SINDRUM II	$< 2 \times 10^{-17}$ Mu2e [50]

TABLE I: Current bounds from measurements of observables with muon initial states.

Process	Current limit	Expected limit 5-10 years		Expected limit 10-20 years
$\mu^+ \to e^+\gamma$	2.4×10^{-12} PSI/MEG (2011)	1×10^{-13} PSI/MEG		1×10^{-14} PSI, Project X
$\mu^+ \to e^+e^-e^+$	1×10^{-12} PSI/SINDRUM-I (1988)	1×10^{-15} Osaka/MuSIC	1×10^{-16} PSI/$\mu 3e$	1×10^{-17} PSI, Project X
$\mu^- N \to e^- N$	7×10^{-13} PSI/SINDRUM-II (2006)	1×10^{-14} J-PARC/DeeMee	6×10^{-17} FNAL/Mu2e	1×10^{-18} J-PARC, Project X

TABLE II: Evolution of the 95% CL limits on the main observables with initial state muons. The expected limits in the 5-to-10 year range are based on running or proposed experiments at existing facilities. The expected bounds in the 10-to-20 year range are based on sensitivity studies using muon rates available at proposed new facilities. The numbers quoted for $\mu^+ \to e^+\gamma$ and $\mu^+ \to e^+e^-e^+$ are limits on the branching fraction. The numbers quoted for $\mu^- N \to e^- N$ are limits on the rate with respect to the muon capture process $\mu^- N \to \nu_\mu N'$. Below the numbers are the corresponding experiments or facilities and the year the current limit was set. Taken from Ref. [1].

Process	5 ab^{-1}	50 ab^{-1}
$\mathcal{B}(\tau \to \mu\,\gamma)$	10×10^{-9}	3×10^{-9}
$\mathcal{B}(\tau \to \mu\,\mu\,\mu)$	3×10^{-9}	1×10^{-9}
$\mathcal{B}(\tau \to \mu\eta)$	5×10^{-9}	2×10^{-9}

TABLE III: Expected 90% CL upper limits on $\tau \to \mu\gamma$, $\tau \to \mu\mu\mu$, and $\tau \to \mu\eta$ with 5 ab^{-1} and 50 ab^{-1} data sets from Belle II and Super KEKB. Taken from Ref. [1].

A. Lepton Flavor Violation in the Anarchic scenario

We begin with $\mu \to e$ transitions and leave comments on τ physics for later.

The transition $\mu \to e\gamma$ can be described at energies smaller than the NP scale by the following higher dimensional operators

$$m_\mu e F_{\mu\nu} \left(\frac{\overline{\mu}_L \sigma^{\mu\nu} e_R}{\Lambda_L^2} + \frac{\overline{\mu}_R \sigma^{\mu\nu} e_L}{\Lambda_R^2} \right), \tag{39}$$

Process	Expected 90%CL upper limit (75 ab^{-1})	3σ Evidence Reach (75 ab^{-1})
$\mathcal{B}(\tau \to \mu\,\gamma)$	1.8×10^{-9}	4.1×10^{-9}
$\mathcal{B}(\tau \to e\,\gamma)$	2.3×10^{-9}	5.1×10^{-9}
$\mathcal{B}(\tau \to \mu\,\mu\,\mu)$	2×10^{-10}	8.8×10^{-10}
$\mathcal{B}(\tau \to eee)$	2×10^{-10}	
$\mathcal{B}(\tau \to \mu\eta)$	4×10^{-10}	
$\mathcal{B}(\tau \to e\eta)$	6×10^{-10}	
$\mathcal{B}(\tau \to \ell K_S^0)$	2×10^{-10}	

TABLE IV: Expected 90% CL upper limits and 3σ discovery reach on $\tau \to \mu\gamma$ and $\tau \to \mu\mu\mu$ and other decays with 75 ab^{-1} at a Super$B$ type machine with a polarized electron beam. Taken from Ref. [1].

which give ($v = 246$ GeV)

$$\mathcal{B}(\mu \to e\gamma) = 96\,\pi^2 e^2 \left(\left| \frac{v}{\Lambda_L} \right|^4 + \left| \frac{v}{\Lambda_R} \right|^4 \right). \tag{40}$$

To estimate the coefficient of these operators in anarchic models we focus on scenarios where dipoles first arise at loop level and make use of naive dimensional analysis. Denoting by Y_* the typical coupling involved in these processes, we expect ($\langle H \rangle = v/\sqrt{2}$)

$$\frac{m_\mu}{\Lambda_L^2} \sim \frac{Y_*^2}{16\pi^2 M_{\rm KK}^2} Y_* F(c_{\ell_2}) F(c_{e_1}) \frac{v}{\sqrt{2}}\,, \quad \frac{m_\mu}{\Lambda_R^2} \sim \frac{Y_*^2}{16\pi^2 M_{\rm KK}^2} Y_* F(c_{\ell_1}) F(c_{e_2}) \frac{v}{\sqrt{2}}, \tag{41}$$

where we ignore complex numbers of order unity. These naive estimates agree with the results found in explicit 5D realizations. In those models the relevant diagrams are generated by loops involving intermediate fermionic KK states, and $Y_*, M_{\rm KK}$ are the 5D Yukawa couplings and KK mass scale respectively.

Another contribution to (39) comes from physics at the cutoff scale, and in a 5D setup can be parametrized by higher dimensional operators in the bulk or localized on the IR. These in general provide counterterms to reabsorb the divergences in the 1-loop diagrams, and are thus expected to be of comparable magnitude by naive dimensional analysis. In actual 5D models, the convergence of the one loop diagrams depends on the localization of the Higgs. For example, for a bulk Higgs the one-loop diagrams are finite and therefore insensitive to the physics at the cutoff. In this latter case, the cutoff effects can naturally be subleading, thus improving predictivity.

From an inspection of (41), and noting that the bounds on $\Lambda_{L,R}$ are numerically the same, follows that the optimal scenarios are those in which

$$\frac{F(c_{\ell_i})}{F(c_{\ell_j})} \sim \frac{F(c_{e_i})}{F(c_{e_j})} \sim \sqrt{\frac{m_i}{m_j}}. \tag{42}$$

We will assume this relation in what follows. Incorporating the unknown $O(1)$ numbers in coefficients $c_{L\mu e, R\mu e}$, we define

$$\frac{m_\mu}{\Lambda_L^2} = c_{L\mu e} \frac{Y_*^2}{16\pi^2} \frac{\sqrt{m_\mu m_e}}{M_{\rm KK}^2}\,, \quad \frac{m_\mu}{\Lambda_R^2} = c_{R\mu e} \frac{Y_*^2}{16\pi^2} \frac{\sqrt{m_\mu m_e}}{M_{\rm KK}^2}. \tag{43}$$

The current bound from the MEG experiment [47], also shown in table I, translates into $\Lambda_{L,R} \gtrsim 860$ TeV or

$$\frac{M_{\rm KK}}{Y_*} \gtrsim 18 \sqrt{|c_{L\mu e}|^2 + |c_{R\mu e}|^2}\ \text{TeV}. \tag{44}$$

The same constraint, shown as a bound on $|c_{L\mu e, R\mu e}|$, is presented in table V.

In Fig. 9 we compare this bound with the results of Ref. [40] obtained for an explicit 5D model with Higgs field with vacuum maximally spread in the bulk ($\nu = 0$). The 5D Yukawas (corresponding to our Y_*) are scanned in the range $|Y_*| \in [0.5, 4]$, and all points reproduce the SM lepton masses. Fig. 9 shows the result for $M_{\rm KK} = 20$ TeV and 80 TeV. We find that in the upper plot only a small fraction of points with small Y_* survives the MEG bound, while for $M_{\rm KK} = 80$ TeV a much larger parameter space becomes available. The figure shows that the naive estimates

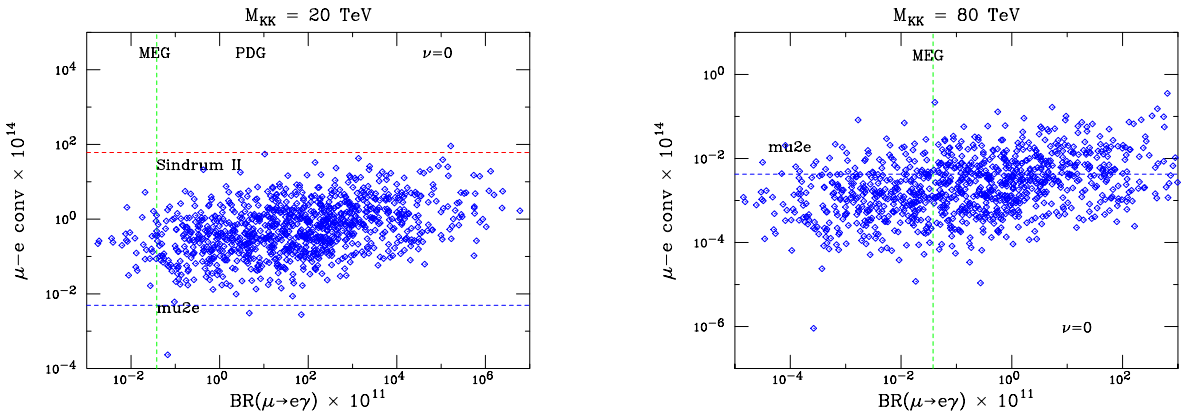

FIG. 9: Scan of the parameter space of a 5D anarchic model [40] with maximally spread Higgs profile ($\nu = 0$) and satisfying Eq. (42), for different Kaluza-Klein mass scales ($M_{KK} = 20$, 80 TeV). The dashed lines indicate the current 90% CL bounds.

Eq. (43) agree pretty well with the numerical results if we take $|c_L| \simeq |c_R| \simeq 3$ in (43) (see Eq.(51) of [40] with $\Delta_{L,R} \sim Y_* F(c_{l,e})$ and $\Delta_2 \sim Y_* v$).

Another important bound on these models arises from the electron EDM. This is generated by the CP-odd component of flavor-diagonal operators analogous to those in Eq. (39), and we can estimate

$$\frac{d_e}{e} = \mathrm{Im}(c_e) \frac{Y_*^2}{16\pi^2} \frac{m_e}{M_{\rm KK}^2}, \tag{45}$$

again with $c_e = \mathcal{O}(1)$. Imposing the 90% CL bound $d_e \lesssim (6.9 \pm 7.4) \times 10^{-28} e$ cm [46] gives $M_{\rm KK}/Y_* \gtrsim (7 - 36)\sqrt{|\mathrm{Im}(c_e)|}$ TeV. This bound has a much larger uncertainty compared to $\mu \to e\gamma$, but demonstrates that both CP and flavor violation are severely constrained in the charged lepton sector.

If CP is maximally violated the muon EDM is expected to be of order $d_\mu \sim d_e m_\mu/m_e \sim 10^{-23} e$ cm $\times (Y_*$ TeV$/M_{\rm KK})^2$, and hence well below present and future bounds for $M_{\rm KK}$ in the TeV range. A similar order of magnitude estimate holds for $(g-2)_\mu$. Electric and magnetic dipole moments of τ are not constraining.

So far we have discussed the effect of dipole operators, and we have seen that the constraints on the NP scale $M_{\rm KK}$ get weaker in weakly coupled theories. The couplings Y_* cannot be taken arbitrarily small, however, because there exist observables that get enhanced in the limit $Y_* \ll 1$. The most relevant such operator is

$$\frac{F(c_{\ell_2})F(c_{\ell_1})}{f^2} \overline{\mu_L} \gamma^\mu e_L \, iH^\dagger \overleftrightarrow{D}_\mu H, \tag{46}$$

with $f \sim M_{\rm KK}/Y_*$, and similarly for the right handed fields with $c_{\ell_i} \to c_{e_i}$. Keeping the fermion masses $\sim Y_* F^2 v$ fixed, it is clear that a small Y_* requires larger mixing parameters $F(c)$, and hence effectively results in larger Wilson coefficients.

Let us now discuss the impact of the above operators. Once the Higgs acquires a vev, Eq. (46) introduces a flavor-changing coupling of the leptons to the Z boson. Integrating out the Z, we obtain 4-fermion operators with the structure $F(c_{\ell_i})F(c_{\ell_j}) \overline{\ell_i} \gamma^\mu \ell_j J_\mu^{(Z)}/f^2$. These are much more important than 4-fermion operators directly generated by the strong dynamics, which are suppressed by an additional factor of $F^2(c)$.

The induced 4-fermion operators contribute to $\ell_i \to \ell_j$ transitions. A stringent bound arises from $\mu \to e$ conversion in matter. Currently, the strongest bounds come from targets of gold and titanium [41], but $R^{Au}_{\mu\to e}$ is more stringent due to a larger coherent conversion. Because this bound equally applies to both chiralities of the leptons we will conservatively assume

$$F(c_{\ell_i}) \sim F(c_{e_i}). \tag{47}$$

The relevant operators can then be written as

$$\frac{c_{ij}}{Y_* f^2} \frac{\sqrt{m_i m_j}}{v} \, \overline{e_i} \gamma^\mu P_{L,R} e_j \, H^\dagger i \overleftrightarrow{D}_\mu H, \tag{48}$$

with c_{ij} complex numbers of order unity. We follow Ref. [44] and write

$$R^{Au}_{\mu\to e} = \left|\frac{c_{e\mu}}{Y_* f^2}\frac{\sqrt{m_e m_\mu}}{v}\right|^2 \left[\left(1-4s_W^2\right)V_N^{(p)} - V_N^{(n)}\right]^2 \frac{m_\mu^5}{\Gamma^N_{\rm capt.}}, \tag{49}$$

where $\Gamma^{Au}_{\rm capt.} = 8.7\times 10^{-18}$ GeV is the capture rate in gold, while $V^{(p)}_{Au}\approx 0.09$ and $V^{(n)}_{Au}\approx 0.1$ are nuclear form factors. The SINDRUM II bound [45] finally gives

$$f\sqrt{Y_*} \gtrsim 2.0\sqrt{|c_{e\mu}|}\ \text{TeV}. \tag{50}$$

The observable $\mu\to ee^+e^-$ is mediated by the same operators (39) and (46), though now with the Z attached to a left and/or right $\bar e\gamma^\mu e$ current. The present bounds on the dipole operators are weaker than those from $\mu\to e\gamma$, while those on the penguin operators (46) are comparable to those from $\mu + Au\to e + Au$, as shown in the table.

We thus see that the most stringent constraints on the anarchic scenarios come from $\mu\to e\gamma$ and $\mu + Au\to e + Au$, and the next most stringent bounds are from the electron EDM and $\mu\to e\bar e e$.

Having derived the most stringent current bounds, let us turn to a discussion of $\tau\to\ell$. The rates for these transitions can be derived by a procedure completely analogous to the one employed above. We therefore skip the details and merely quote the results.

For $\tau\to\ell\gamma$ we find

$$\mathcal{B}(\tau\to\ell\gamma) = \mathcal{B}(\mu\to e\gamma)\frac{(|c_{L\tau\ell}|^2+|c_{R\tau\ell}|^2)}{(|c_{L\mu e}|^2+|c_{R\mu e}|^2)}\frac{m_\ell}{m_\tau}\frac{m_\mu}{m_e}\times\mathcal{B}(\tau\to\ell\bar\nu\nu). \tag{51}$$

Up to $O(1)$ numbers, the largest branching fraction is $\mathcal{B}(\tau\to\mu\gamma)\sim\mathcal{B}(\mu\to e\gamma)$, and is already bounded to be below $\sim 5.7\times 10^{-13}$. From this we conclude that, unless some cancellation among order one numbers occurs, anarchic theories satisfying the $\mu\to e\gamma$ bound will not show up in $\tau\to\ell\gamma$ decays.

On the other hand, the channels $\tau\to\ell\bar f f$ are more promising:

$$\mathcal{B}(\tau\to\ell\bar f f)\sim\mathcal{B}(\mu\to e\bar e e)\frac{m_\tau m_\ell}{m_\mu m_e}\times\mathcal{B}(\tau\to\ell\bar\nu\nu), \tag{52}$$

where $\bar f f$ could be a lepton as well as a quark pair of the same flavor. (Processes involving flavor-violating pairs $\bar f f'$ are not mediated by Z exchange and are suppressed by additional powers of $F(c)\ll 1$, which make them completely negligible.) Plugging in some representative numbers, we find $\mathcal{B}(\tau\to\mu\bar f f)\sim(10^2-10^3)\times\mathcal{B}(\mu\to e\bar e e)$. Given the present bound on $\mathcal{B}(\mu\to e\bar e e)$ we argue that future B-factories will be able to probe exotic τ decays with these topologies. The expected improvement in the measurement of $\mathcal{B}(\mu\to e\bar e e)$ is much more dramatic, though, and we therefore expect that among these channels $\mu\to e\bar e e$ will remain the most efficient probe of anarchic scenarios. Yet, we remark that $\mathcal{B}(\tau\to\mu\bar f f)$ will become a complementary test of these models.

Operator	$\lvert\mathrm{Re}(c)\rvert$ $\quad$ $\lvert\mathrm{Im}(c)\rvert$	Observable
$c\frac{Y_*^2}{16\pi^2}\frac{m_e}{M_{\rm KK}^2}\ \bar e\sigma^{\mu\nu}eF_{\mu\nu}e_{L,R}$	— $\quad$ $1.1\ \left(\frac{m_\rho/Y}{10\ \text{TeV}}\right)^2$	electron EDM
$c\frac{Y_*^2}{16\pi^2}\frac{\sqrt{m_e m_\mu}}{M_{\rm KK}^2}\ \bar\mu\sigma^{\mu\nu}eF_{\mu\nu}e_{L,R}$	$0.31\ \left(\frac{m_\rho/Y}{10\ \text{TeV}}\right)^2$	$\mu\to e\gamma$
”	$3.7\ \left(\frac{m_\rho/Y}{10\ \text{TeV}}\right)^2$	$\mu\to ee^+e^-$
$\frac{c}{Y_* f^2}\frac{\sqrt{m_e m_\mu}}{v}\ \bar e\gamma^\mu\mu_{L,R}\,H^\dagger i\overleftrightarrow{D}_\mu H$	$0.25\ \left(\frac{\sqrt{Y}f}{1\ \text{TeV}}\right)^2$	$\mu(Au)\to e(Au)$
”	$0.38\ \left(\frac{\sqrt{Y}f}{1\ \text{TeV}}\right)^2$	$\mu\to ee^+e^-$

TABLE V: Upper bounds on the dimensionless coefficients c of the operators in the first column, assuming that m_ρ, Y are real. See the text for details.

VIII. CONCLUSIONS

In the first part of this note, we computed the impact of resonances in a complete model of warped extra dimensions on flavor changing observables in the quark sector. Assuming anarchic order one Yukawa couplings, these models can be described by one localization parameter and the new physics scale $M_{\rm KK}$. Universal bounds from electroweak precision data and the measurement of the Higgs mass constrain this mass scale to $M_{\rm KK} \gtrsim 5$ TeV in a minimal model with only a SM bulk gauge group and $M_{\rm KK} \gtrsim 2$ TeV if a custodial $SU(2)_R \times SU(2)_L$ bulk symmetry protects the T parameter from large corrections. Since the lightest KK gluon mode has a mass of $m_{\rm G^{(1)}} \approx 2.5\, M_{\rm KK}$ and has small couplings to light quarks, it is challenging to observe this state in direct collider searches. We emphasized that precise measurements of flavor violation in $K \to \pi\bar{\nu}\nu$ as proposed by the ORKA collaboration together with future LHCb measurements have the potential to determine the quark localization parameters. A future precise measurement of the correlated quantities $\mathcal{B}(K_L \to \mu^+\mu^-)$ and $\mathcal{B}(K^+ \to \pi^+\bar{\nu}\nu)$ can identify the helicity structure of new physics contributions and therefore allows to identify the underlying bulk gauge group. New limits on these quantities serve as a signpost for future collider searches for KK resoances. We derived the correlation between flavor and collider observables and translated them into projected bounds at the 14 TeV LHC, a luminosity upgrade of the 14 TeV LHC, as well as a potential 33 TeV upgrade and a future 100 TeV pp machine.

In the second part of this note, we discussed the effects in charged lepton flavor observables in models with warped extra dimensions. We calculated the parametric dependence of the new physics contribution to electric dipole moments, $\mu \to ee^+e^-$, $\mu \to e\gamma$, and $\mu \to e$ on the Yukawa couplings, localization parameters and $M_{\rm KK}$. The latter two observables, $\mu \to e\gamma$ and $\mu \to e$, provide the most stringent bounds and are already sensitive to very high KK scales of $M_{\rm KK} > 20$ TeV for anarchic order one Yukawa matrices. The proposed next generation of experiments from the Mu2e and MEG collaborations will probe warped models of flavor in the lepton sector up to $M_{\rm KK} \gtrsim 80$ TeV in the anarchic case and consequentially determine possible flavor structures in the lepton sector if the KK scale is much lower. Finally we discussed corrections to τ decays in Randall-Sundrum models and concluded that the current as well as expected future bounds are generically less constraining than the light lepton flavor observables.

IX. ACKNOWLEDGEMENTS

Fermilab is operated by Fermi Research Alliance, LLC under Contract No. De-AC02-07CH11359 with the United States Department of Energy. Some of the authors (MB, FG, LW and FY) want to thank KITP Santa Barbara for warm hospitality and support during completion of this work. This research is supported in part by the National Science Foundation under Grant No. NSF PHY11-25915. KA is supported by the National Science Foundation under NSF Grant No. PHY-0968854. MB acknowledges the support of the Alexander von Humboldt Foundation. FG acknowledges support by the Swiss National Foundation under contract SNF 200021-143781. SL is supported by the National Research Foundation of Korea(NRF) grant funded by the Korea government(MEST) N01120547. LV was supported in part by NSF Grant No. PHY-0968854, by the NSF Grant No. PHY-0910467, and by the Maryland Center for Fundamental Physics.

Appendix A: Numerical Input

Paramter	Value	Reference
κ_L	$(2.231 \pm 0.013) \cdot 10^{-10}\,(\lambda/0.225)^8$	[51]
κ_+	$(0.5173 \pm 0.0025) \cdot 10^{-10}\,(\lambda/0.225)^8$	[51]
$\Delta_{\rm EM}$	-0.003	[51]
m_{B_d}	5.2796 GeV	[42]
τ_{B_d}	(1.519 ± 0.007) ps	[42]
f_{B_d}	(190.5 ± 4.2) MeV	[43]
m_{B_s}	5.3667 GeV	[42]
τ_{B_s}	(1.516 ± 0.011) ps	[42]
f_{B_s}	(227.7 ± 4.5) MeV	[43]

TABLE VI: Parameters used in the calculations in Section IV.

[1] J. L. Hewett, H. Weerts, R. Brock, J. N. Butler, B. C. K. Casey, J. Collar, A. de Govea and R. Essig *et al.*, "Fundamental Physics at the Intensity Frontier," arXiv:1205.2671 [hep-ex].

[2] C. Csaki, A. Falkowski and A. Weiler, "The Flavor of the Composite Pseudo-Goldstone Higgs," JHEP **0809**, 008 (2008) [arXiv:0804.1954 [hep-ph]].

[3] K. Agashe, G. Perez and A. Soni, Phys. Rev. D **71**, 016002 (2005) [hep-ph/0408134].

[4] S. Casagrande, F. Goertz, U. Haisch, M. Neubert and T. Pfoh, JHEP **0810**, 094 (2008) [arXiv:0807.4937 [hep-ph]].

[5] M. Bauer, S. Casagrande, U. Haisch and M. Neubert, JHEP **1009**, 017 (2010) [arXiv:0912.1625 [hep-ph]].

[6] K. Agashe, R. Contino, L. Da Rold and A. Pomarol, Phys. Lett. B **641**, 62 (2006) [hep-ph/0605341].

[7] S. Casagrande, F. Goertz, U. Haisch, M. Neubert and T. Pfoh, JHEP **1009**, 014 (2010) [arXiv:1005.4315 [hep-ph]].

[8] C. D. Froggatt and H. B. Nielsen, Nucl. Phys. B **147**, 277 (1979).

[9] J. A. Bagger, K. T. Matchev and R. J. Zhang, Phys. Lett. B **412**, 77 (1997) [arXiv:hep-ph/9707225].

[10] M. Ciuchini *et al.*, JHEP **9810**, 008 (1998) [arXiv:hep-ph/9808328].

[11] A. J. Buras, M. Misiak and J. Urban, Nucl. Phys. B **586**, 397 (2000) [arXiv:hep-ph/0005183].

[12] G. Beall, M. Bander and A. Soni, Phys. Rev. Lett. **48**, 848 (1982).

[13] F. Gabbiani, E. Gabrielli, A. Masiero and L. Silvestrini, Nucl. Phys. B **477**, 321 (1996) [arXiv:hep-ph/9604387].

[14] J. Santiago, JHEP **0812**, 046 (2008) [arXiv:0806.1230 [hep-ph]].

[15] M. Redi and A. Weiler, JHEP **1111**, 108 (2011) [arXiv:1106.6357 [hep-ph]].

[16] C. Csaki, G. Perez, Z. 'e. Surujon and A. Weiler, Phys. Rev. D **81**, 075025 (2010) [arXiv:0907.0474 [hep-ph]].

[17] M. Bauer, R. Malm and M. Neubert, Phys. Rev. Lett. **108**, 081603 (2012) [arXiv:1110.0471 [hep-ph]].

[18] M. Baak, M. Goebel, J. Haller, A. Hoecker, D. Ludwig, K. Moenig, M. Schott and J. Stelzer, Eur. Phys. J. C **72**, 2003 (2012) [arXiv:1107.0975 [hep-ph]].

[19] O. Gedalia, G. Isidori and G. Perez, Phys. Lett. B **682**, 200 (2009) [arXiv:0905.3264 [hep-ph]].

[20] NA62 Collaboration, `http://na62.web.cern.ch/na62`

[21] KOTO collaboration, `http://koto.kek.jp`

[22] A. S. Kronfeld, R. S. Tschirhart, U. Al-Binni, W. Altmannshofer, C. Ankenbrandt, K. Babu, S. Banerjee and M. Bass *et al.*, arXiv:1306.5009 [hep-ex].

[23] BELLE II Collaboration, `http://belle2.kek.jp`

[24] Aaij *et al.* [LHCb Collaboration], arXiv:1307.5024 [hep-ex].

[25] F. Goertz and T. Pfoh, Phys. Rev. D **84** (2011) 095016 [arXiv:1105.1507 [hep-ph]].

[26] A. V. Artamonov *et al.* [E949 Collaboration], Phys. Rev. Lett. **101**, 191802 (2008) [arXiv:0808.2459 [hep-ex]].

[27] D. M. Straub, arXiv:1302.4651 [hep-ph].

[28] B. A. Dobrescu and F. Yu, Phys. Rev. D **88**, 035021 (2013) [arXiv:1306.2629 [hep-ph]].

[29] F. Yu, arXiv:1308.1077 [hep-ph].

[30] K. Kong and F. Yu, arXiv:1308.1078 [hep-ph].

[31] F. Mescia, C. Smith and S. Trine, JHEP **0608**, 088 (2006) [arXiv:hep-ph/0606081].

[32] M. Misiak and J. Urban, Phys. Lett. B **451**, 161 (1999) [hep-ph/9901278].

[33] G. Buchalla and A. J. Buras, Nucl. Phys. B **548**, 309 (1999) [hep-ph/9901288].

[34] C. Csaki, C. Delaunay, C. Grojean and Y. Grossman, JHEP **0810** (2008) 055 [arXiv:0806.0356 [hep-ph]].

[35] M. -C. Chen, K. T. Mahanthappa and F. Yu, Phys. Rev. D **81**, 036004 (2010) [arXiv:0907.3963 [hep-ph]].

[36] M. -C. Chen, K. T. Mahanthappa and F. Yu, AIP Conf. Proc. **1200**, 623 (2010) [arXiv:0909.5472 [hep-ph]].

[37] K. Agashe, T. Okui and R. Sundrum, "A Common Origin for Neutrino Anarchy and Charged Hierarchies," Phys. Rev. Lett. **102**, 101801 (2009) [arXiv:0810.1277 [hep-ph]].

[38] B. Keren-Zur, P. Lodone, M. Nardecchia, D. Pappadopulo, R. Rattazzi and L. Vecchi, Nucl. Phys. B **867**, 429 (2013) [arXiv:1205.5803 [hep-ph]].

[39] S. J. Huber, Nucl. Phys. B **666**, 269 (2003) [hep-ph/0303183].

[40] K. Agashe, A. E. Blechman and F. Petriello, Phys. Rev. D **74**, 053011 (2006) [hep-ph/0606021].

[41] K. Nakamura *et al.* [Particle Data Group Collaboration], J. Phys. G G **37** (2010) 075021.

[42] J. Beringer *et al.* [Particle Data Group Collaboration], Phys. Rev. D **86**, 010001 (2012).

[43] G. Colangelo et al. (FLAG), *in preparation*

[44] V. Cirigliano, B. Grinstein, G. Isidori and M. B. Wise, Nucl. Phys. B **728**, 121 (2005), hep-ph/0507001. V. Cirigliano and B. Grinstein, Nucl. Phys. B **752**, 18 (2006), hep-ph/0601111. T. Suzuki, D. F. Measday and J. P. Roalsvig, Phys. Rev. C **35**, 2212 (1987). R. Kitano, M. Koike and Y. Okada, Phys. Rev. D **66**, 096002 (2002) [Erratum-ibid. D **76**, 059902 (2007)], hep-ph/0203110.

[45] U. Bellgardt *et al.* [SINDRUM Collaboration], Nucl. Phys. B **299**, 1 (1988).

[46] B. C. Regan, E. D. Commins, C. J. Schmidt and D. DeMille, Phys. Rev. Lett. **88**, 071805 (2002).

[47] J. Adam *et al.* [MEG Collaboration], "New constraint on the existence of the $\mu \to e\gamma$ decay," arXiv:1303.0754 [hep-ex].

[48] A. M. Baldini *et al.* [MEG Collaboration], "MEG Upgrade Proposal," arXiv:1301.7225[hep-ex].

[49] A. Blondel *et al.* [Mu3e Collaboration], "Research Proposal for an Experiment to Search for the Decay $\mu \to eee$" arXiv:1301.6113[hep-ex].

[50] R. J. Abrams *et al.* [Mu2e Collaboration], "Mu2e Conceptual Design Report," arxiv:1211.7019[hep-ex].

[51] F. Mescia and C. Smith, "Improved estimates of rare K decay matrix-elements from Kl3 decays," Phys. Rev. D **76**, 034017 (2007) [arXiv:0705.2025 [hep-ph]].